

## OPTICALLY INDUCED DIVACANCY REORIENTATIONS IN SILICON

R.H. VAN DER LINDE AND C.A.J. AMMERLAAN  
NATUURKUNDIG LABORATORIUM, UNIVERSITEIT VAN AMSTERDAM,  
VALCKENIERSTRAAT 65, AMSTERDAM-C, THE NETHERLANDS

### ABSTRACT

Divacancies were produced in phosphorus doped silicon by irradiation at room temperature with 1.5 MeV electrons. Divacancies are accommodated in the host silicon lattice in twelve distinct orientations with different vacancy-vacancy direction and Jahn-Teller distortion. The Si-G7 EPR spectrum is associated with the paramagnetic negative charge state of the defect. Illumination with linearly polarized light with wavelength around 3.6  $\mu\text{m}$  at low temperatures induces reorientations of the divacancies. The population of some orientations is enhanced at the expense of the other orientations. This is monitored directly in the EPR spectrum. A model to explain the light induced changes is proposed, and predictions based on the model are compared with the experimental results.

### I. THE DIVACANCY IN SILICON

A stereographic model of the divacancy in silicon, as given in figure 1, illustrates that the defect consists of a pair of vacancies on adjacent lattice sites. Silicon crystallizes in the diamond lattice. Divacancies in silicon are stable and immobile defects at room temperature. They are

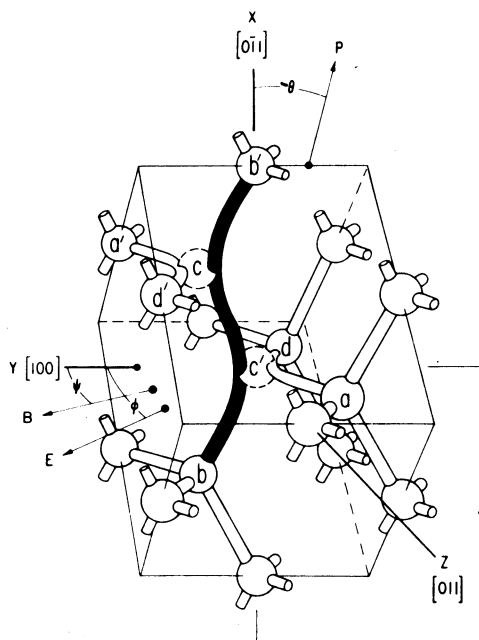


FIGURE 1. Model of the divacancy in silicon. Dashed circles labeled *c* and *c'* represent vacancy sites. Defect orientation *cb* is shown. The extended bond is more heavily drawn.

nearest neighbours.

The divacancy gives rise to deep levels in the bandgap of the semiconductor silicon. Depending on the position of the Fermi level the defect will assume one of the four possible charge states  $V_2^{2-}$ ,  $V_2^-$ ,  $V_2^0$ , and  $V_2^+$ . Only in the states  $V_2^+$

among the predominant and therefore most extensively studied radiation defects<sup>1-4</sup>. In our case the divacancies were produced by room temperature irradiation with 1.5 MeV electrons to a dose of  $3 \times 10^{18}$  electrons per  $\text{cm}^2$ . By the creation of a divacancy the bonds with its six nearest neighbour atoms - *a*, *b*, *d*, *a'*, *b'*, and *d'* in figure 1 - are broken. The lattice around the defect relaxes and new bonds are formed as indicated in the figure. To a first approximation the electronic structure is well described by linear combinations of the six  $sp^3$ -hybridized dangling bond orbitals on the

## OPTICALLY INDUCED DIVACANCY REORIENTATIONS IN SILICON

and  $V_2^-$  the number of electrons on the defect is odd and the divacancy behaves as an  $S = \frac{1}{2}$  paramagnetic center. Here we report a study of the divacancy in the singly negatively charged state  $V_2^-$ . The EPR spectrum associated with it is known as Si-G7<sup>1</sup>. It is observed in n-type silicon when after irradiation the Fermi level has dropped to below  $E_c - 0.4$  eV. Our silicon was phosphorus doped, its room temperature resistivity of 0.03 Ohm.cm corresponds to a donor concentration of  $7 \times 10^{17}$  atoms per  $\text{cm}^3$ .

In the unrelaxed silicon lattice the divacancy has pointgroup  $\bar{3}m$  ( $D_{3d}$ ) symmetry. In the negative charge state  $V_2^-$  the upper level, which has double orbital degeneracy, is only partly filled with three electrons. Consequently a Jahn-Teller distortion will occur to lower the energy. The resulting defect symmetry is pointgroup  $2/m$  ( $C_{2h}$ ).

As a consequence of the low defect symmetry the divacancy can be accommodated in the silicon lattice in twelve different orientations. The vacancy-vacancy axis can be directed along each of the four  $\langle 111 \rangle$  bond directions in the crystal. For each of these cases three different Jahn-Teller distortions are possible. In the adopted way of labeling divacancy orientations the first letter specifies the direction of the second vacancy as seen from the vacancy site  $c'$  in figure 1. The second letter gives the atoms lying in the plane of reflection of the defect. The unpaired electron primarily resides in the extended bond formed from the orbitals centered on these atoms.

The main character of the EPR spectrum of the divacancy is described by the g-tensor. For a center of low symmetry the Zeeman splitting is anisotropic resulting in an angle dependent effective g-value. Figure 2 shows the pattern of g-values formed by the twelve divacancy orientations for the

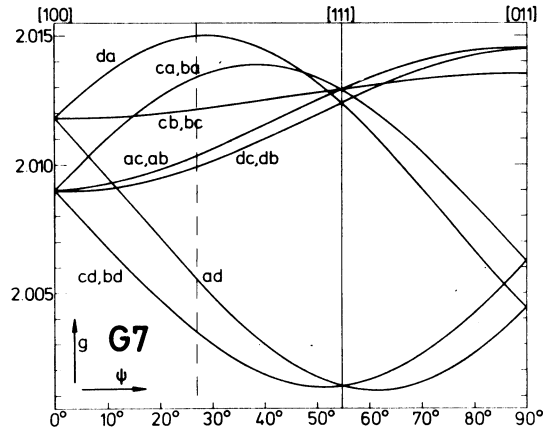


FIGURE 2.  $g$ -Values versus crystalline orientation of  $\vec{B}$  in the  $(0\bar{1}1)$  plane for the Si-G7 spectrum, associated with the negative divacancy in silicon. Curves are labeled with the corresponding defect orientations.

usual experimental conditions where  $\vec{B}$  is chosen in the  $(0\bar{1}1)$  plane. For reasons of symmetry some resonances coincide in pairs, e.g.  $(bd,cd)$  and  $(bc,cb)$ . Two pairs of lines  $(ab,ac)$  and  $(db,dc)$  unfortunately almost coincide over the entire angular region in the  $(0\bar{1}1)$  plane. At K-band frequencies these components are not resolved experimentally. Therefore, in practice, instead of the twelve lines which can be distinguished in principle, only six lines corresponding to single, two-fold, or four-fold multiplicities of divacancy orientations are observed. For our measurements we have selected for best resolution an angular setting of  $\vec{B}$  of  $27^\circ$  off the  $[100]$  direction towards  $[011]$ . This is indicated by the dashed vertical line in figure 2.

## OPTICALLY INDUCED DIVACANCY REORIENTATIONS IN SILICON

### II. OPTICALLY INDUCED DIVACANCY ALIGNMENT, EXPERIMENTAL

By irradiation of silicon several optical absorption bands in the infrared are induced. Bands at the wavelengths 1.8  $\mu\text{m}$ , 3.3  $\mu\text{m}$ , and 3.9  $\mu\text{m}$  were associated with the divacancy in particular charge states<sup>2</sup>. It was observed that illumination with polarized light in the absorption bands causes reorientations of the divacancies, resulting in a reduction of the absorption coefficient<sup>3</sup>. In our experiment the light induced divacancy alignment was observed in and quantitatively monitored by the EPR spectrum of the defect. The present study is equivalent to one described earlier for the positive charge state  $V_2^+$  of the divacancy<sup>4</sup>.

In our experimental set-up the irradiated silicon sample, approximately 20x2x2 mm<sup>3</sup> in size, was mounted with its long dimension, the crystallographic  $[0\bar{1}1]$  direction, along the axis of the TE011 microwave cavity. The sample was illuminated on the top, the  $(0\bar{1}1)$  face, with infrared light in a wavelength band of  $(3.6 \pm 0.2)$   $\mu\text{m}$ . The light was linearly polarized, with the rotatable polarization angle  $\phi$  of  $\vec{E}$  in the  $(0\bar{1}1)$  plane, using a Brewster angle polarizer mounted immediately above the cavity. The sample is kept at low enough temperatures to avoid thermal anneal of the light induced changes.

The redistribution of the divacancies among the twelve possible orientations in the silicon lattice, as induced by the infrared illumination, were monitored by recording the G7 EPR spectra. As explained earlier, for best resolution  $\vec{B}$  was taken off the  $[100]$  direction in the  $(0\bar{1}1)$  plane. Magnetic field scans of 10 mT in 150 seconds were made. We used our K-band superheterodyne spectrometer, microwave frequency 22.7 GHz, which was tuned to observe the dispersion

R. H. VAN DER LINDE AND C. A. J. AMMERLAAN

part  $\chi'$  of the susceptibility, in phase with the applied 19 Hz magnetic field modulation. The sample temperature was kept at 8.8 K.

Typical divacancy EPR spectra are shown in figure 3. The central part 3(a) of the figure represents the spectrum before any illumination of the sample at low tempera-

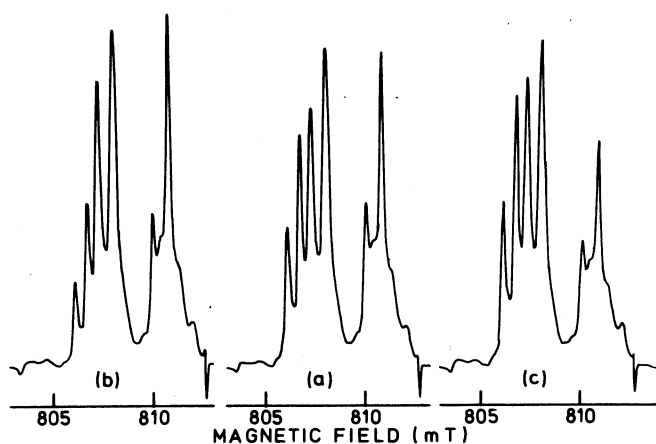


FIGURE 3. EPR spectra for  $V_2^-$  in Si for  $\vec{B} // [100] + 27^\circ$  in the  $(0\bar{1}1)$  plane, microwave frequency = 22.7 GHz,  $T = 8.8$  K. (a) the spectrum before illumination, (b) after illumination,  $\lambda = 3.6 \mu\text{m}$ ,  $\vec{E} // [100] - 58^\circ$  in the  $(0\bar{1}1)$  plane, (c) similar to (b), but  $\vec{E} // [100] + 40^\circ$ .

tures, and therefore corresponds to the situation where the divacancies are equally distributed over all possible orientations. Six resonance lines are observed, of which, from left to right, the amplitude is proportional to the number of divacancies in the orientations  $da$ ,  $(ba, ca)$ ,  $(bc, cb)$ ,  $(ab, ac) + (db, dc)$ ,  $ad$ , and  $(bd, ed)$ , respectively.

## OPTICALLY INDUCED DIVACANCY REORIENTATIONS IN SILICON

Changes in the spectrum reflecting the light induced divacancy redistributions for two different angles of the polarization vector  $\vec{E}$  are illustrated by parts (b) and (c) of figure 3. The alignment effect depends on the angle of polarization and may even reverse sign. For example, the intensity of the *da* spectral component is reduced by  $\vec{E} // [100] - 58^\circ$ , while it has grown in amplitude for  $\vec{E} // [100] + 40^\circ$ . On the other hand, the number of divacancies in the (*bc,cb*) orientations is seen to have increased under illumination with both directions of polarization.

In a sample with random divacancy distribution alignment starts to be induced as soon as the light is switched on. The initial alignment rate is proportional to the light intensity. After a length of time a saturation value of the alignment is obtained. Because of low light intensities it took in our case illumination times of 1 to 2 hours to reach this steady state. The maximum alignment effect, i.e. after saturation is established, is plotted in figure 4 as function of the angle of polarization of the  $\vec{E}$  vector in the (0 $\bar{1}1$ ) plane. Several features as displayed by this figure will be discussed in the next section of this paper, when comparing the experimental results with the predictions of the theoretical model.

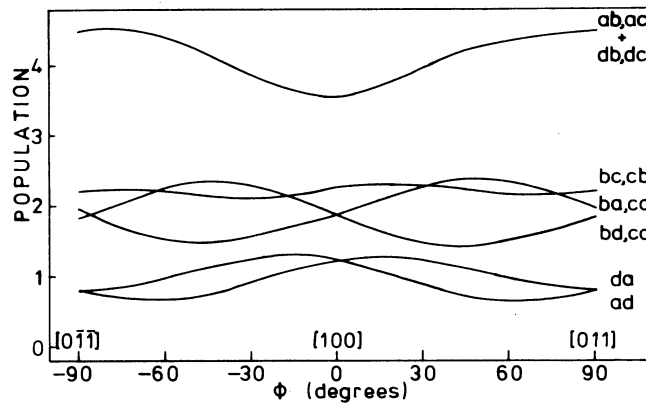


FIGURE 4. Saturation populations of the various divacancy orientations after illumination with polarized light with  $\vec{E}$  in the  $(0\bar{1}1)$  plane, for a wavelength  $\lambda = (3.6 \pm 0.2) \mu\text{m}$ .

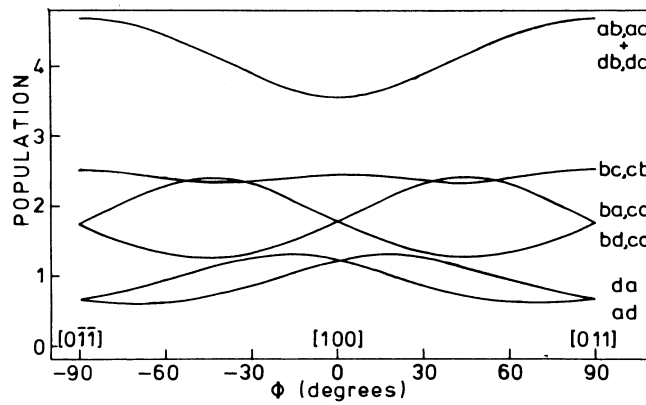


FIGURE 6. Saturation populations calculated for a transition with dipole moment in the reflection plane of the divacancy, angle  $\theta = -15^\circ$ .

## OPTICALLY INDUCED DIVACANCY REORIENTATIONS IN SILICON

### III. OPTICALLY INDUCED DIVACANCY ALIGNMENT, THEORETICAL MODEL

Inspection of the phase relations between the induced alignment of the various divacancy orientations, as shown in figure 4, suggests that sums of populations within the Jahn-Teller triplets are constant. For reasons explained earlier only two pairs of triplets, consisting of the orientations  $ad$ ,  $da$ ,  $(ab, ac)$ , and  $(db, dc)$  on one hand, and the remaining orientations on the other hand, can be distinguished experimentally. The total populations of these pairs of triplets, when plotted versus the angle of the  $\vec{E}$  vector, show a marked constancy in comparison with the variations of the individual components. From this experimental fact we conclude that the light affects only the electronic orientational degree of freedom of the divacancy, i.e. the Jahn-Teller distortion direction. The atomic orientation of the defect, which is the direction of the vacancy-vacancy axis, does not change under illumination. For this reason in the model only reorientations within the Jahn-Teller triplets are considered.

The alignment model for divacancies of the triplet consisting of the orientations  $ab$ ,  $ac$ , and  $ad$  is shown schematically in figure 5. By absorbing a photon the divacancy is excited into a state with higher energy, different electronic wavefunction, and distortion. The excitation probability  $M^2$  will depend on the angle between the electric field vector  $\vec{E}$  of the polarized light and the transition dipole moment  $\vec{P}$ :

$M_{ij} = \cos(\vec{E}, \vec{P}_{ij})$ . Components of the transition dipole

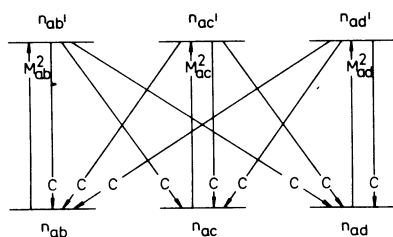


FIGURE 5. Model for the optically induced divacancy reorientations within the Jahn-Teller triplet consisting of the defect orientations  $ab$ ,  $ac$ , and  $ad$ .

moment are given by  $P_x = \langle f|x|i\rangle$ , etc. The excitation probabilities will therefore depend on the direction of  $\vec{E}$  with respect to the defect and will be different for different divacancy orientations. On the other hand it is assumed that de-excitation from a specific excited orientation occurs with equal probability to each of the three ground state configurations of the triplet. This is symbolized by the equal de-excitation rate constants  $C$  in figure 5. The model predicts an increase of the populations of orientations which are hard to excite, compensated by a loss of divacancies in the easily excited orientations.

To put the model on a more quantitative basis the angle  $\theta$  defined by  $\text{tg}\theta \equiv \langle f|y|i\rangle/\langle f|x|i\rangle$  is introduced;  $|i\rangle$  and  $|f\rangle$  represent initial and final electronic states of the defect, respectively. The angle between  $\vec{E}$  and  $[100]$  in the  $(0\bar{1}1)$  plane is specified by  $\phi$ . From symmetry arguments it follows that the transition dipole moment  $\vec{P}$  is a vector which either lies in the plane of reflection of the divacancy, called the XY plane, or is perpendicular to this plane

OPTICALLY INDUCED DIVACANCY REORIENTATIONS IN SILICON

and points in the Z direction. It appears that the latter type of transitions do lead nowhere to any agreement with the experimental results and they are therefore left out of further consideration. The excitation probabilities for XY dipole transitions are given by:

$$\begin{aligned} M_{ab} &= -\cos \theta \cos \phi / \sqrt{2} + \cos \theta \sin \phi / 2 + \sin \theta \sin \phi / \sqrt{2}, \\ M_{ac} &= M_{ab}, \\ M_{ad} &= \cos \theta \sin \phi - \sin \theta \cos \phi. \end{aligned}$$

Similar expressions hold for the divacancy orientations belonging to the other Jahn-Teller triplets. Rate equations like

$$dn_{ab}/dt = -M_{ab}^2 n_{ab} + (M_{ab}^2 n_{ab} + M_{ac}^2 n_{ac} + M_{ad}^2 n_{ad})/3$$

lead to steady state solutions like

$$n_{ab} = 3M_{ac}^2 M_{ad}^2 / (M_{ab}^2 M_{ac}^2 + M_{ac}^2 M_{ad}^2 + M_{ad}^2 M_{ab}^2).$$

The model as outlined above predicts variations of the populations ranging from complete extinction to a maximum three-fold increase. Experimentally a smaller alignment effect is observed. This may be due to practical deficiencies like a non-ideal polarizer, the randomizing effect of depolarized scattered light in the sample or stray light in the microwave cavity. To improve the agreement between the experimental results and the calculated populations we have similarly introduced an adjustable smoothing parameter in the model. With this feature added and taking  $\theta = -15^\circ$  calculated saturation values for the populations of the divacancy orientations are shown in figure 6.

Comparing the experimental result in figure 4 with the theoretical result in figure 6 the general similarity of oscillating curves with a shape that clearly deviates from simple sinusoidal behaviour is apparent. The population of orientation *ad* has its maximum for  $\phi = -15^\circ$ , both

R. H. VAN DER LINDE AND C. A. J. AMMERLAAN

experimentally and theoretically. For orientation *da* the maximum occurs at  $\phi = +15^\circ$  in both cases. All curves oscillate around their equilibrium pre-illumination value, with the exception of the divacancy orientations (*bc,cb*) for which an increase of the population is found, both experimentally and theoretically, over the entire angular region of  $\vec{E}$ . The period of the oscillations is  $180^\circ$ . Again, the curve for (*bc,cb*) constitutes the exception by having the double angular frequency. From this agreement between the experimental results and the calculated ones in these several aspects we conclude that the model is realistic. The optical transition responsible for the divacancy reorientations has XY dipole character, with an angle  $\theta$  of  $-15^\circ$  between the transition dipole moment  $\vec{P}$  and the closest  $\langle 110 \rangle$  crystallographic direction.

#### REFERENCES

1. G.D.Watkins and J.W.Corbett, Phys.Rev., 138, A543 (1965).
2. L.J.Cheng, J.C.Corelli, J.W.Corbett, and G.D.Watkins, Phys.Rev., 152, 761 (1966).
3. L.J.Cheng and P.Vajda, Phys.Rev., 186, 816 (1969).
4. C.A.J.Ammerlaan and G.D.Watkins, Phys.Rev., B5, 3988 (1972).